

# Diffuse Galactic Light in a Field of Translucent Cloud MBM32 at High Galactic Latitude

K. KAWARA,<sup>1</sup> K. SANO,<sup>1</sup> N. IENAKA,<sup>1</sup> Y. MATSUOKA,<sup>2</sup> H. SAMESHIMA,<sup>3</sup> AND S. OYABU<sup>2</sup>

<sup>1</sup>*Institute of Astronomy, University of Tokyo, Japan*

<sup>2</sup>*Graduate School of Science, Nagoya University, Japan*

<sup>3</sup>*Institute of Space and Astronautical Science, JAXA, Japan*

## ABSTRACT

We have conducted multi-color optical imaging toward a high-Galactic cloud, and correlated the intensity of diffuse optical light to the  $100\ \mu\text{m}$  intensity  $S(100\ \mu\text{m})$ . A  $\chi^2$ -minimum technique was employed to fit a linear function of  $S(100\ \mu\text{m})$  to the observed correlation and derive the slope parameter of the best fit-function  $\Delta(\text{DGL})/\Delta(100\ \mu\text{m})$ . Combining our slope values and published ones, we show that the slope parameter values vary from cloud to cloud. Because the slope parameter decreases as  $S(100\ \mu\text{m})$  increases, we suggest that a non-linear DGL model including a negative quadratic term of  $S(100\ \mu\text{m})$  be fitted to the observed correlation.

## 1. INTRODUCTION

The extragalactic background light (EBL) from the optical to near-infrared is the cumulative emission of galaxies, intergalactic gas and stars, AGNs as well as emission from other exotic sources not common at the present epoch such as pregalactic objects (population III) and decaying unknown-particles. The claimed detections of the EBL at near-infrared wavelengths give 3–10 times greater values than the integrated intensities expected from galaxy counts. This may indicate that the EBL is dominated by a new, unknown emission component, or that the measurements of those claimed values are biased by incomplete subtraction of foreground emission such as zodiacal light and diffuse galactic light (DGL).

Based on our recent work by [Ienaka et al. \(2013\)](#), we present a study of the DGL, one of the important foregrounds, which is scattered light by interstellar dust grains illuminated by the interstellar radiation field (ISRF).

## 2. OBSERVATIONS

The optical data toward translucent cloud MBM32 at  $(l, b) = (147, 41)$  have been acquired at four photometric bands,  $B$ ,  $g$ ,  $V$ , and  $R$ . The observations were conducted on the 105cm Schmidt telescope at Kiso observatory<sup>1</sup> using the 2KCCD camera with  $2048 \times 2048$  pixels. The Sun and the Moon were more than 35 degrees below the horizon during the observations. The field of view of the camera is  $50' \times 50'$  with a pixel scale of  $1''.5\ \text{pixel}^{-1}$ . The average seeing was  $\sim 3''.3$ . The area of high-quality is approximately  $45' \times 40'$ , smaller than the field of view of the camera due to using dithering.

The left panel in [Figure 1](#) indicates the observed field by the white square superimposed on the *IRAS/DIRBE*  $100\ \mu\text{m}$  map ([Schlegel et al. 1998](#)), and the right shows optical pseudo color mages. In order to reduce the effects of large-scale

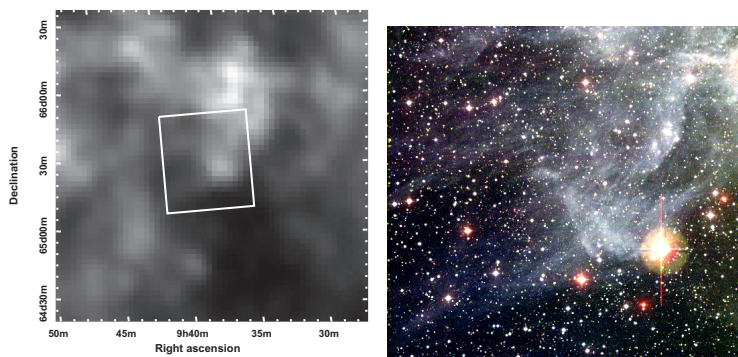


**Figure 1.** *Left:* Optical field at MBM32 superimposed on the *IRAS/DIRBE*  $100\ \mu\text{m}$  map ([Ienaka et al. 2013](#)). The solid square represents the observed field. *Right:* The optical pseudo color image synthesized from  $B/g/VR$  imaging. North is up, east to the left. The field is approximately  $45' \times 40'$ .

<sup>1</sup> Kiso observatory is operated by the Institute of Astronomy, the University of Tokyo

KAWARA ET AL.

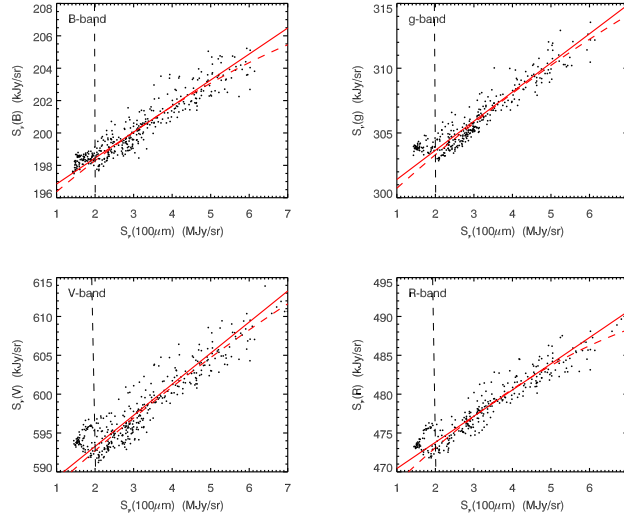


**Figure 2.** Correlation of the intensity of the diffuse optical light against  $100\ \mu\text{m}$  intensity (Ienaka et al. 2013). The red solid lines represent the linear functions recovered from the  $\chi^2$  minimum analysis, while the red dashed lines represent the quadratic functions.

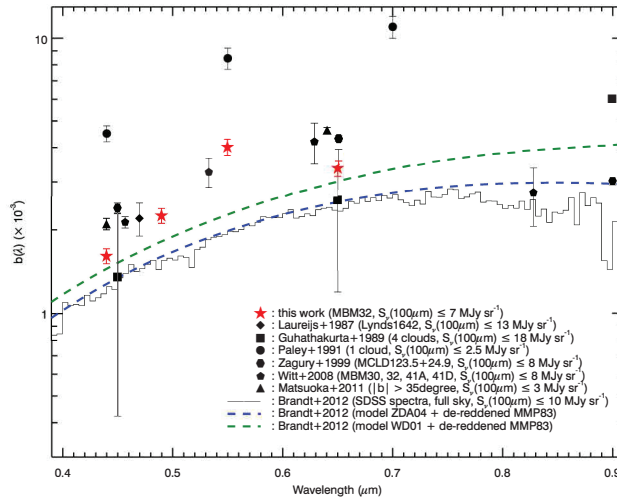


**Figure 3.** The correlation slopes  $b(\lambda) = \Delta S_v(\lambda)/\Delta S_v(100\ \mu\text{m})$  as a function of wavelengths (Ienaka et al. 2013).

non-uniformity in the flat-fielding, we observed the field at two different telescope attitudes by flipping the telescope around the right ascension axis in such a way that the difference in hour angle is 180 degrees, thereby rotating the image plane on the detector by 180 degrees. The diffuse optical light component was measured by rejecting stars and galaxies from the images.

### 3. RESULTS

Figure 2 plots the intensity of diffuse optical light,  $S_v(\lambda)$ , as a function of  $100\ \mu\text{m}$  intensity,  $S_v(100\ \mu\text{m})$ .  $S_v(\lambda)$  clearly correlates with  $S_v(100\ \mu\text{m})$  at all the bands. We now fit to the data a linear function defined as:  $S_v(\lambda) = a(\lambda) + b(\lambda)S_v(100\ \mu\text{m})$ , where the slope parameter at wavelength  $\lambda$  is  $b(\lambda) = \Delta S_v(\lambda)/\Delta S_v(100\ \mu\text{m})$ , and the constant parameter  $a(\lambda)$  represents components independent of the DGL (i.e., atmospheric airglow, zodiacal light, and the EBL). A minimum  $\chi^2$  analysis was performed to obtain  $a(\lambda)$  and  $b(\lambda)$ . Figure 3 plots  $b(\lambda)$  as a function of wavelength along with the published data, which are taken from Witt et al. (2008), Matsuoka et al. (2011), Brandt & Draine (2012), Laureijs et al. (1987), Guhathakurta & Tyson (1989), Paley et al. (1991), and Zagury et al. (1999), as well as the model spectrum from Brandt & Draine (2012). The figure indicates that  $b(\lambda)$  varies by a factor of 3–4.

### 4. DISCUSSION

Figure 4 (Ienaka et al. 2013) illustrates  $b(\lambda)$  as a function of  $S_v(100\ \mu\text{m})$ , which indicates that  $b(\lambda)$  decreases as  $S_v(100\ \mu\text{m})$  increases. Sujatha et al. (2010) reported that  $b(\lambda)$  at far-UV wavelengths exponentially decreases with

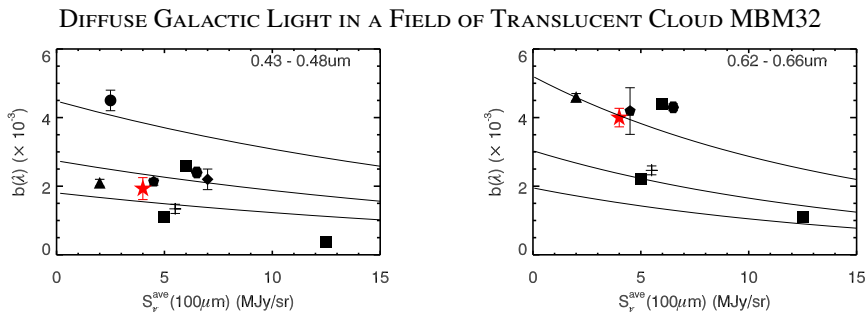


**Figure 4.**  $b(\lambda)$  against  $S_V(100 \mu\text{m})$  by Ienaka et al. (2013).  $S_V^{\text{ave}}(100 \mu\text{m})$  refers to the representative average in the individual  $S_V(100 \mu\text{m})$  ranges. The legend for the points is the same as in Figure 2, except for the crosses which are the averaged spectroscopy data from Brandt & Draine (2012). The lines represent the relation expected for albedos  $\omega_V = 0.6, 0.7,$  and  $0.8$  from lower to upper (Ienaka et al. 2013).

$S_V(100 \mu\text{m})$  increasing. It is likely that such decrease is due to the absorption by dust along the line of sight. The optical depth in the optical is much less than in the far-UV, thus the  $b(\lambda)$  decrease appears to be linear against  $S_V(100 \mu\text{m})$  at the optical. Therefore, it would be appropriate to fit a functional form of  $S_V(\lambda) = a(\lambda) + b(\lambda)S_V(100 \mu\text{m}) - c(\lambda)S_V(100 \mu\text{m})^2$  to the observed correlation.

## REFERENCES

- Brandt, T. D., & Draine, B. T. 2012, 744, 129  
 Guhathakurta, P., & Tyson, J. A. 1989, ApJ, 346, 773  
 Ienaka, N., Kawara, K., Matsuoka, Y., et al. 2013, ApJ, 767, 80  
 Laureijs, R. J., Mattila, K., & Schnur, G. 1987, A&A, 184, 269  
 Matsuoka, Y., Ienaka, N., Kawara, K., & Oyabu, S. 2011, ApJ, 736, 119  
 Paley, E. S., Low, F. J., McGraw, J. T., et al. 1991, ApJ, 376, 335  
 Schlegel, D. J., Finkbeiner, D. P., & Davis, M. 1998, ApJ, 500, 525  
 Sujatha, N. V., Murthy, J., Suresh, R., et al. 2010, 723, 1549  
 Witt, A. N., Mandel, S., Sell, P. H., et al. 2008, ApJ, 679, 497  
 Zagury, F., Boulanger, F., & Banchet, V. 1999, A&A, 352, 645